resemble those for the C_3 group, i.e. $(Y,EuO)_2S$, and consequently YOOH should be counted with this group. However, it has earlier been shown on grounds of crystal structure that (RE)OOH compounds belong to the C_4 group.[31]

Acknowledgment. We wish to express our gratitude to Dr. Pierre Porcher and Dr. Christian Chateau for fruitful discussions.

Registry No. LaOOH, 12195-45-8; GdOOH, 12160-84-8; LuOOH, 12141-10-5; YOOH, 12026-07-2; Eu^{3+}, 22541-18-0.

(31) Dexpert, H.; Lemaitre-Blaise, M.; Caro, P. *React. Solids, Proc. Int. Symp., 7th* **1972**, 758.

(32) Leavitt, R. P.; Gruber, J. B.; Chang, N. C.; Morrison, C. A. *J. Chem. Phys.* **1982**, *76*, 4775.

(33) Huang, J.; Loriers, J.; Porcher, P. *J. Solid State Chem.* **1982**, *43*, 87.

Contribution from the Department of Chemistry, Texas A&M University, College Station, Texas 77843

Theoretical Studies of Bridging-Ligand Effects in Quadruply Bonded Dichromium(II) Compounds

RANDALL A. KOK and MICHAEL B. HALL*

Received May 30, 1984

Generalized molecular orbital (GMO) and configuration interaction (CI) calculations are reported for $Cr_2(O_2CH)_4$ and $Cr_2((NH)_2CH)_4$ at various Cr–Cr bond lengths. The results show a bond shortening of 0.48 Å when the formato ligands are replaced by amino iminato ligands. Analysis of the CI wave function shows that the stronger donating ligand, $(NH)_2CH$, causes the Cr atomic orbitals to expand and thereby increases the Cr–Cr overlaps. Thus, the inductive effect of the bridging ligand may be an important factor in determining the Cr–Cr bond length.

Introduction

Quadruply bonded dichromium(II) compounds exhibit an unusually wide range of Cr–Cr bond lengths from 1.828 to 2.541 Å.[1] With only a few exceptions these compounds can be divided into two groups.[2] The first group of compounds have Cr–Cr bond lengths that range from 2.283 to 2.541 Å. This group of compounds is characterized by four carboxylato ligands and some kind of interaction in the axial position, either in the form of solvent molecules or of a molecular structure in which the carboxylato units are arranged in infinite chains with intermolelar O···Cr interactions. The second group of compounds have Cr–Cr bond lengths of less than 1.90 Å. This second group is characterized by ligands derived from weaker acids and usually has no axial interactions.

The cause of this wide range in Cr–Cr bond lengths has been the subject of many experimental[2-15] and theoretical[16-24] investigations in recent years. In general, the wide variability of bond lengths has been attributed to two possible causes.[5] The first of these is the effect of axial ligand interaction, which has been investigated experimentally. Cotton, Ilsley, and Kaim reported[2] a series of compounds containing zero, one, and two tetrahydrofuran ligands in the axial position and very similar bridging ligands. As expected, the Cr–Cr bond length increased from 1.873 to 2.023 to 2.221 Å in this series. More recent work by Cotton and Wang,[15] on a series of 14 compounds in which the axial and bridging ligands were varied systematically, led them to conclude that the presence or absence of axial ligands was the determining factor in the Cr–Cr bond length.

The second possible cause, the inductive effect of the bridging ligand, has not been as thoroughly investigated experimentally. Berry and co-workers[25] did report a study of the correlation of chromium–chromium bond lengths with chromium orbital ionization energies. In the compounds they studied, the chromium–chromium separation followed the electron-withdrawing or -releasing properties of the bridging ligands. Also, Cotton and Wang[15] have reported structures of five tetrakis(carboxylato)dichromium compounds, all with axial pyridine groups, in which the bridging ligand was varied. This series does show a change of 0.2 Å in the Cr–Cr bond length over the series of compounds. However, no *systematic* experimental approach has resolved whether or not the chromium–chromium bond length in unsolvated dichromium tetracarboxylates would be in the supershort range. This is due in large part to difficulties in synthesizing these compounds. Thus, the question of the bond length in such complexes remains open.

We felt that a theoretical approach to this question might provide some insight into the competing effects on the Cr–Cr bond length. We have recently reported preliminary results on tetra-

(1) Cotton, F. A; Walton, R. A. "Multiple Bonds Between Metal Atoms"; Wiley: New York, 1982; reference therein.
(2) Cotton, F. A.; Ilsley, W.H.; Kaim, W. *J. Am. Chem. Soc.* **1980**, *102*, 3464.
(3) Cotton, F. A.; DeBoer, B. G.; LaPrade, M. D.; Pipal, J. R.; Ucko, D. A. *Acta Crystallogr., Sect. B: Struct. Crystallogr. Cryst. Chem.* **1971**, *B27*, 1664.
(4) Cotton, F. A.; Rice, C. E.; Rice, G. W. *J. Am. Chem. Soc.* **1977**, *99*, 4704.
(5) Cotton, F. A.; Extine, M. W.; Rice, G. W. *Inorg. Chem.* **1978**, *17*, 176.
(6) Cotton, F. A.; Rice, G. W. *Inorg. Chem.* **1978**, *17*, 688.
(7) Cotton, F. A.; Rice, G. W. *Inorg. Chem.* **1978**, *17*, 2004.
(8) Bino, A.; Cotton, F. A.; Kaim, W. *J. Am. Chem. Soc.* **1979**, *101*, 2056.
(9) Bino, A.; Cotton, F. A.; Kaim, W. *Inorg. Chem.* **1979**, *18*, 3030.
(10) Bino, A.; Cotton, F. A.; Kaim, W. *Inorg. Chem.* **1979**, *18*, 3566.
(11) Cotton, F. A.; Ilsley, W.H.; Kaim, W. *J. Am. Chem. Soc.* **1980**, *102*, 3475.
(12) Cotton, F. A.; Thompson, J. L. *Inorg. Chem.* **1981**, *20*, 1292.
(13) Cotton, F. A.; Mott, G. N. *Organometallics* **1982**, *1*, 302.
(14) Cotton, F. A.; Falvello, L. R.; Han, S.; Wang, W. *Inorg. Chem.* **1983**, *22*, 4106.
(15) Cotton, F. A.; Wang, W., submitted for publication in *Nouv. J. Chim.*
(16) Garner, C. D.; Hillier, I. H.; Guest, M. F.; Green, J. C.; Coleman, A. W. *Chem. Phys. Lett.* **1976**, *41*, 91.
(17) Cotton, F. A.; Stanley, G. G. *Inorg. Chem.* **1977**, *16*, 2668.
(18) Guest, M. F.; Hillier, I. H.; Garner, C. D. *Chem. Phys. Lett.* **1977**, *48*, 587.
(19) Benard, M. *J. Am. Chem. Soc.* **1978**, *100*, 2354.
(20) Benard, M. *J. Chem. Phys.* **1979**, *71*, 2546.
(21) Atha, P. M.; Hillier, I. H.; Guest, M. F. *Mol. Phys.* **1982**, *46*, 437.
(22) De Mello, P. C.; Edwards, W. D.; Zerner, M. C. *J. Am. Chem. Soc.* **1982**, *104*, 1440.
(23) Kok, R. A.; Hall, M. B. *J. Am. Chem. Soc.* **1983**, *105*, 676.
(24) Wiest, R.; Benard, M. *Chem. Phys. Lett.* **1983**, *98*, 102.
(25) Berry, M.; Garner, C. D.; Hillier, I. H.; MacDowell, A. A.; Walton, I. B. *Chem. Phys. Lett.* **1980**, *70*, 350.

0020-1669/85/1324-1542$01.50/0

kis(formato)dichromium and tetrakis(formamidato)dichromium at 2.1 Å.[23] These results showed that, at a given bond length, the 3d orbitals in tetrakis(formamidato)dichromium had a much larger overlap in the Cr–Cr bonding region than those in tetrakis(formato)dichromium. This increase in the overlap leads to a stronger Cr–Cr bond. These results also indicated that the nature of the bridging ligand strongly affects the strength of the quadruple bond and may, in fact, determine whether or not axial ligands will bond. We concluded that if a tetrakis(carboxylato) species without any axial ligands could be synthesized, a small decrease in the quadruple bond length might occur. However, this decrease would not be enough to move this compound into the group of compounds with bond lengths less than 1.90 Å.

Since that time, Wiest and Benard[24] have reported ab initio calculations on $Cr_2(O_2CH)_4$, $Cr_2(NHCHO)_4$, and $Cr_2(O_2CH)_4(H_2O)_2$. They performed configuration interaction calculations on their Hartree–Fock wave functions for these three compounds and found that adding the axial water molecules to the formato species causes a change of only 0.05 Å in the equilibrium bond length but changing the bridging ligand from formato to formamidato causes a decrease of 0.5 Å in the equilibrium bond length.

There is a problem, however, in this calculation. The lower symmetry of $Cr_2(NHCHO)_4$ causes the $d\pi$ orbitals to localize on one chromium or the other during the calculation, leading to drastic changes in the Hartree–Fock potential energy curve as compared to the curve for a symmetrically bridged species like $Cr_2(O_2CH)_4$.[26] Because of this "broken-symmetry" solution for $Cr_2(NHCHO)_4$, it is not clear how much of the large difference in the equilibrium bond lengths for $Cr_2(O_2CH)_4$ and $Cr_2(NHCHO)_4$ is due to this calculational problem and how much is due to the actual inductive effects of the different bridging ligands.

In order to avoid the problem associated with broken-symmetry solutions and examine the actual bridging ligand effects, we did calculations on two compounds with the same symmetry: tetrakis(formato)dichromium, $Cr_2(O_2CH)_4$, and tetrakis(aminomethaniminato)dichromium, $Cr_2((NH)_2CH)_4$. These two compounds represent the two broad classes of quadruply bonded dichromium(II) compounds that have very different equilibrium bond lengths. By examining these two compounds, both of which have D_{4h} symmetry, we hope to look directly at bridging-ligand effects in these compounds.

Theoretical Section

Generalized Molecular Orbital Theory and Configuration Interaction. The generalized molecular orbital approach[27] is a limited multiconfiguration–self-consistent field (MC–SCF) calculation. It provides an optimized set of primary orbitals for configuration interaction (CI) calculations and needs only modest addition effort beyond that needed for the Hartree–Fock–Roothaan (HF) or standard molecular orbital (MO) approach. In the standard MO approach for a $2n$-electron closed-shell molecule, the MO's, which have been expanded in a basis set, are divided into doubly occupied and unoccupied sets as

$$(\phi_1 \cdots \phi_n)^2(\phi_{n+1} \cdots \phi_m)^0 \qquad (1)$$

In the GMO approach the previously doubly occupied orbitals are divided into a doubly occupied set and a strongly occupied set, while the previously unoccupied orbitals are divided into a weakly occupied set and an unoccupied set. These four sets of orbitals may be thought of as molecular core, valence, valence correlating, and virtual orbitals, respectively. The electronic configuration in the GMO framework may be written as

$$(\phi_1 \cdots)^2(\cdots \phi_n)^x(\phi_{n+1} \cdots)^y(\cdots \phi_m)^0 \qquad (2)$$

It is this shell structure, in which the orbitals are treated in sets with all orbitals in a set having equal occupation numbers, that led to the use of the name generalized molecular orbital theory.

Details of the computational procedure have been given previously.[27] The choice of orbitals for each of the GMO sets is usually straightforward. In this case the strongly occupied set consisted of the four orbitals in the qudruple bond, the σ, π_x, π_y, and δ orbitals, while the weakly occupied set consisted of their antibonding counterparts, the σ^*, π_x^*, π_y^*, and δ^* orbitals. All the orbitals were kept doubly occupied except for those involved in the quadruple bond. For the eight electrons in the quadruple bond, the GMO wave function consisted of the dominant single determinant (σ^2, π_x^2, π_y^2, δ^2) plus all paired double excitations, from these bonding orbitals to their antibonding counterparts (σ^*, π_x^*, π_y^*, δ^*), weighted equally. Application of the variation principle yielded a set of primary orbitals (σ, π_x, π_y, δ, σ^*, π_x^*, π_y^*, δ^*) in which the weakly occupied ones (σ^*, π_x^*, π_y^*, δ^*) were optimized to correlate with the strongly occupied ones (σ, π_x, π_y, δ). The determination of the GMO orbitals was then followed by a full CI calculation in this restricted orbital space.

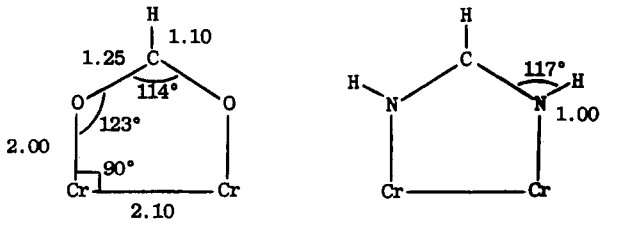

Figure 1. Structure of dichromium model compounds. The bond lengths and angles given for the tetrakis(formato) species apply to the amino iminato species as well.

From the CI calculation, we derived the natural orbitals (NO's) and their occupation numbers by diagonalizing the one-electron density matrix.[28] If we assume that the same NO's and occupation numbers would be obtained from a generalized valence-bond (GVB) calculation[29] over this orbital space, we can then generate pseudogeneralized valence-bond (PGVB) pairs. We have given details of this procedure previously.[30]

Geometry. The bond lengths and angles for the two systems are shown in Figure 1 and are based on average values compiled from a number of known quadruply bonded dichromium species.[3-7] The symmetry of both $Cr_2(O_2CH)_4$ and $Cr_2((NH)_2CH)_4$ is D_{4h}. In calculation of the potential energy curves, the bridging ligand was kept rigid and only the Cr–Cr bond length was changed. The Cr–Cr bond length was varied from 1.9 to 2.7 Å at 0.2-Å intervals for $Cr_2(O_2CH)_4$ and from 1.7 to 2.3 Å at 0.2-Å intervals for $Cr_2((NH)_2CH)_4$.

Basis. The basis functions employed in this study were obtained from a least-squares fit of a linear combination of Gaussians to near-Hartree–Fock–quality Slater type functions.[31] The program GEXP processes the functions from the 1s outward, keeping each orbital of higher n quantun number orthogonal to the previous ones. This procedure results in an efficiently nested representation of the function.[32] In this study, the number of Gaussians used for each function was increased until the integral error of the fit[33] was less than 2×10^{-3} for valence functions and 5×10^{-4} for core functions. It was found that three Gaussians per atomic orbital were sufficient, except for the Cr 3d, where five Gaussians were used.

A fully contracted basis set was used for all the atoms in the ligands. The Cr basis set consisted of a set of (10s7p5d) primitive Gaussian-type orbitals contracted to [4s3p2d] on each atom. The most diffuse component of the 3d was split off to form a double-ζ representation. The Cr basis was also augmented by an s function, exponent 0.10, and a p function, exponent 0.15.

Calculations. All calculations were carried out on the Texas A&M University Amdahl 470V/6 and V/7 computers and the Chemistry Department VAX 11/780 computer. The integrals and the Hartree–Fock–Roothaan[34] calculations were done with the ATMOL3 system of programs.[35] The GMO calculations were done with a program written by M.B.H. The CI calculations were done with a package written by Dr.

(26) Benard, M. *J. Chem. Phys.* **1979**, *71*, 2546.
(27) (a) Hall, M. B. *Chem. Phys. Lett.* **1979**, *61*, 461. (b) Hall, M. B. *Int. J. Quantum Chem.* **1978**, *14*, 613. (c) Hall, M. B. *Int. J. Quantum Chem., Quantum Chem. Symp.* **1979**, *No. 13*, 195. (d) Hall, M. B. In "Recent Developments and Applications of Multiconfiguration Hartree-Fock Methods"; Dupuis, M., Ed.; National Technical Information Science: Springfield, VA, 1981; NRCC Proceedings No. 10, p 31.
(28) (a) Lowdin, P. O. *Phys. Rev.* **1955**, *97*, 1474. (b) Bingel, W. A.; Kutzelnigg, W. *Adv. Quantum Chem.* **1970**, *5*, 201. (c) Davidson, E. R. *Rev. Mod. Phys.* **1972**, *44*, 451.
(29) Goddard, W. A., III; Dunning, T. H., Jr.; Hunt, W. J.; Hay, P. J. *Acc. Chem. Res.* **1973**, *6*, 368.
(30) Chinn, J. W., Jr.; Hall, M. B. *Inorg. Chem.* **1983**, *22*, 2759.
(31) (a) Clementi, E. *J. Chem. Phys.* **1964**, *40*. (b) Clementi, E. *IBM J. Res. Dev.* **1965**, *9*, 2 and its supplement ("Tables and Atomic Functions"). (c) Roetti, C.; Clementi, E. *J. Chem. Phys.* **1974**, *60*, 3342.
(32) Marron, M. T.; Handy, N. C.; Parr, R. G.; Silverstone, H. G. *Int. J. Quantum Chem.* **1970**, *4*, 245.
(33) Stewart, R. F. *J. Chem. Phys.* **1970**, *52*, 431.
(34) Roothaan, C. C. J. *Rev. Mod. Phys.* **1951**, *23*, 69.
(35) Hillier, I. H.; Saunders, V. R.; Guest, M. F. ATMOL3 System, Chemistry Department, University of Manchester, Manchester, U.K., and SRC Laboratory, Daresbury, U.K.

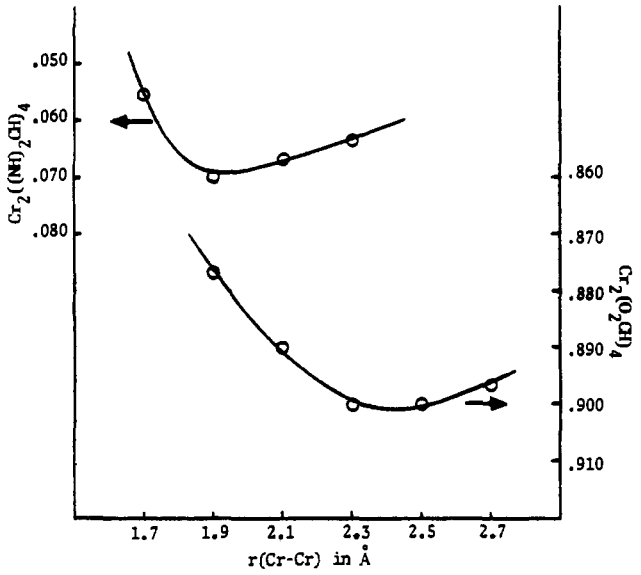

Figure 2. Potential energy curves for $Cr_2((NH)_2CH)_4$ and $Cr_2(O_2CH)_4$. The scale on the left side plus 2655 hartrees represents the absolute value of the CI energy for $Cr_2((NH)_2CH)_4$. The scale on the right side plus 2811 hartrees represents the absolute value of the CI energy for $Cr_2(O_2CH)_4$. The minimum for these curves are 1.93 andd 2.41 Å, respectively.

C. T. Corcoran, Dr. J. M. Norbeck, and Professor P. R. Certain. This package, which was written for a Harris computer, was modified by T. E. Taylor and M. B. Hall for the Amdahl 470 and VAX 11/780 computers.

The wave functions were used in the program MOPLOT[36] to generate total electron density and orbital maps. These maps were then used to help interpret the interactions between the two chromium atoms and the bridging ligands. The maps were drawn by the program CONTOUR[37] on a Xerox 9700 electronic printing system with a graphics package called Electronic Printer Image Construction.

Results and Discussion

Potential Energy Curves. The geometries for the compounds studied are shown in Figure 1. The potential energy curves for $Cr_2(O_2CH)_4$ and $Cr_2((NH)_2CH)_4$ are shown in Figure 2 at the CI level of calculation. Serious errors are often present in simple HF calculations, especially in calculations on the compounds under discussion. In all the compounds, the HF calculation predicts equilibrium bond lengths that are much too short and a potential energy well with sides that are much too steep. In compounds such as these, where HF calculations do so poorly, CI calculations are necessary in order to determine reliable bond lengths and force constants. The GMO–CI calculation not only lowers the total energy but also flattens the potential energy curve, resulting in the shallow potential well found by other researchers.[19,22,24] This shallow potential energy well is one of the most frequently sited reasons for the wide range of Cr–Cr bond lengths since small changes in the compounds can create large changes in the Cr–Cr bond length without changing the total energy significantly. Also, the GMO–CI calculation increases the equilibrium bond length. The minimum for the HF curve for $Cr_2(O_2CH)_4$ occurs at 1.56 Å, while the minimum for the CI curve occurs at 2.41 Å. The minimum for the HF curve for $Cr_2((NH)_2CH)_4$ occurs at 1.18 Å, while the minimum for the CI curve occurs at 1.93 Å.

Analysis of Wave Function. One way to examine the origin of the Cr–Cr bond shortening upon going from the tetrakis(formato) species to the tetrakis(amino iminato) species is to see how the nature of the bridging ligand affects the wave function of the compounds. These results are shown in Table I and are given for the respective compounds at the calculated point closest to their predicted equilibrium bond length. At the top of Table I, we have listed the orbital occupation numbers for the two systems. As can be seen, the number of electrons in the bonding orbitals increases upon going from $Cr_2(O_2CH)_4$ to $Cr_2((NH)_2CH)_4$, especially in the π orbital. In the second part, we have listed the square of the coefficients of the configurations that comprise the ground-state wave functions. For $Cr_2(O_2CH)_4$, the quadruply bonded configuration is only about 12% of the ground-state wave function. Other configurations with less than four bonds contribute almost as much to the ground-state wave function. On the other hand, for $Cr_2((NH)_2CH)_4$, the quadruple bond makes up almost 50% of the ground-state wave function. In the third part, we have listed the pseudogeneralized valence-bond orbital overlap values.[29] These values were calculated from our natural orbital occupation numbers.[30] These overlap values give an indication of how "molecular" or "atomic" these orbitals are. Orbitals with low overlap values have almost as many electrons in their antibonding component as in their bonding component. Thus, these orbitals do not contribute very much to a strong bond and are very atomic in character. Orbitals with high overlap values, however, are strongly bonding and are very molecular in character. The higher overlap values for $Cr_2((NH)_2CH)_4$ again indicate that this compound has a stronger quadruple bond than $Cr_2(O_2CH)_4$. This same pattern is seen if you compare these properties for the two compounds at a bond length between their equilibrium bond lengths, such as 2.1 Å, although the magnitude of the differences is smaller.

Table I. Comparison of Quadruple-Bond Strength

	$Cr_2(O_2CH)_4$[a]	$Cr_2((NH)_2CH)_4$[b]
Orbital Occupations		
σ	1.47	1.73
π	2.44	3.33
δ	1.18	1.51
δ^*	0.82	0.49
π^*	1.56	0.67
σ^*	0.53	0.27
Important Configurations[c]		
$\sigma^2\pi^4\delta^2$	0.117	0.482
$\sigma^2\pi^4\delta^{*2}$	0.054	0.085
$\sigma^2\pi^2\delta^2\pi^{*2}$	0.083	0.094
$\pi^4\delta^2\sigma^{*2}$	0.017	0.019
GVB Orbital Overlap Values		
σ	0.25	0.44
π	0.11	0.38
δ	0.09	0.28
Ratio of d-Orbital Coefficients		
σ	0.201	0.179
π	0.200	0.229
δ	0.211	0.247

[a] Values for molecule at 2.3 Å. [b] Values for molecule at 1.9 Å. [c] Values represent the sum of the square of the coefficients corresponding to different spin components of the same configuration.

Orbital Plots. The strongly and weakly occupied orbitals of $Cr_2(O_2CH)_4$ from our GMO–CI calculation are shown in Figure 3. Only one of the two perpendicular π and π^* orbitals is shown. As expected, the antibonding orbitals have a node between the metal centers, while the bonding orbitals do not. These orbital maps provide a graphic illustration of what electron correlation does to the total energy and electron density. In standard Hartree–Fock theory, all the strongly occupied orbitals have two electrons in them and the weakly occupied orbitals have none. The HF calculation does not take into account the dynamic electron–electron repulsion that results from the proximity of two electrons in the same orbital. When excitations are allowed to antibonding orbitals, orbitals that contain nodes between the metal

(36) Lichtenberger, D. L. Ph.D. Dissertation, University of Wisconsin, Madison, WI, 1974. Program available from: Quantum Chemistry Program Exchange, Indiana University, Bloomington, IN 47401; Program 284.
(37) An in-house program that uses CONREC, a special smoothing routine for drawing contours, developed at the National Center for Atmospheric Research (NCAR), Boulder, CO, and adapted for use on the Amdahl 470V/6 by T. Reid, Data Processing Center, Texas A&M University.
(38) Benard, M.; Coppens, P.; DeLucia, M. L.; Stevens, E. D. *Inorg. Chem.* **1980**, *19*, 1924.

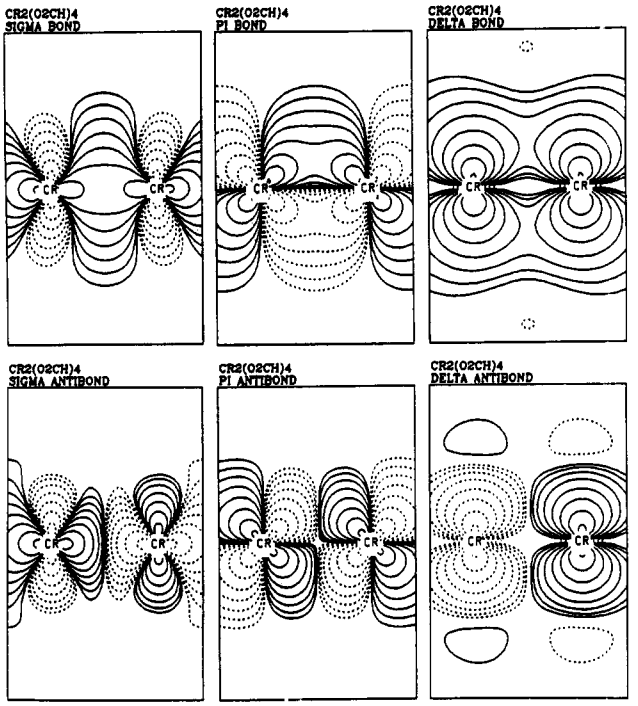

Figure 3. Strongly and weakly occupied natural orbitals of $Cr_2(O_2CH)_4$. The top three orbital maps represent the σ, π, and δ orbitals, respectively, while the bottom three orbital maps represent their antibonding counterparts.

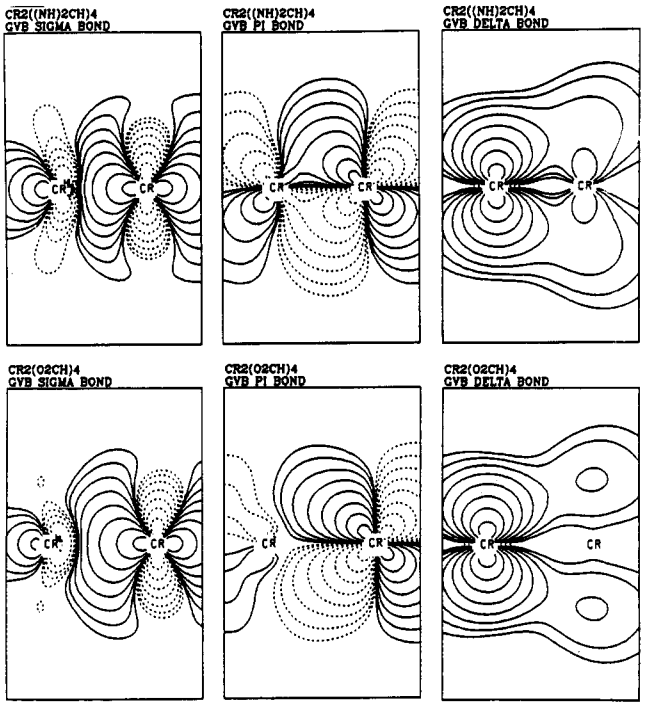

Figure 4. Pseudo-GVB orbitals for $Cr_2((NH_2)CH)_4$ and $Cr_2(O_2CH)_4$. As the molecule dissociates, these pseudo-GVB orbitals evolve into pure atomic orbitals. Thus, at the equilibrium bond length, the degree of delocalization of these orbitals is a measure of the strength of the bond.

centers mix into the ground state. This allows the electrons to spend part of the time on opposite centers, thereby reducing the electron–electron repulsion and lowering the total energy. In other words, CI allows the electrons to separate spatially, and it increases the probability that if one electron is on one Cr atom, the other electron of the pair will be on the other Cr atom.

In Figure 4, we have plotted pseudo-GVB orbitals derived from the proper linear combination of our strongly and weakly occupied orbitals. This combination will produce two orbitals, which are

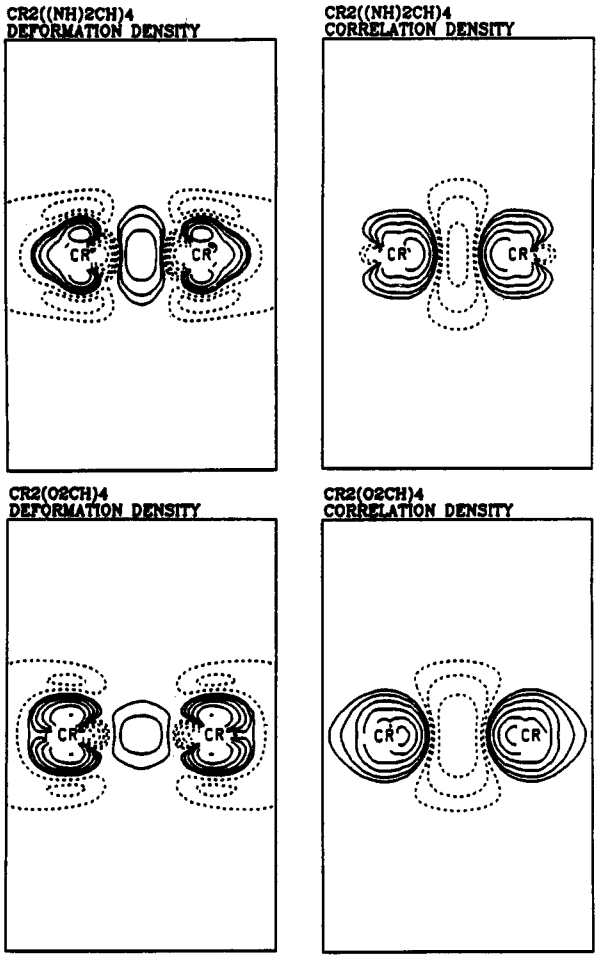

Figure 5. Electron deformation density maps for $Cr_2((NH)_2CH)_4$ and $Cr_2(O_2CH)_4$. The outermost contour has a value of $^1/_{256}$ e au^{-3} or 0.026 e Å^{-3}. This solid or dotted line represents the smallest positive or largest negatve contour, respectively. Adjacent contours differ by a factor of 2. The left maps represent the difference between the total electron density distribution and spherical ground-state atomic densities for both compounds. The right maps represent the difference between the GMO–CI and HF total electron density maps for both compounds.

mirror images of each other and contain one electron each. Only one of the two linear combinations is shown. As the molecule dissociates, these pseudo-GVB orbitals evolve into pure atomic orbitals. Thus, at the equilibrium bond length, the degree of delocalization of these orbitals is a measure of the strength of the bond. In the case of $Cr_2((NH)_2CH)_4$ all three orbitals are spread over both Cr centers, indicating orbitals that are molecular in character. In contrast, the orbitals for $Cr_2(O_2CH)_4$, especially the π and δ, are more localized on only one Cr center, indicating orbitals that are almost atomic in character. Again, this emphasizes the differences in the electronic structure of the quadruple bond in these two compounds.

Strength of the Quadruple Bond. All three methods shown in Table I for analyzing the CI wave function indicate that $Cr_2((NH)_2CH)_4$ has the stronger quadruple bond, with $Cr_2(O_2CH)_4$ considerably weaker. One explanation for this effect can be found by examining the radial extent of the d functions on the Cr atoms. At the bottom of Table I, we have listed the ratio of the coefficient of the diffuse d orbital to that of the contracted d orbital. For the π and δ orbitals, $Cr_2((NH)_2CH)_4$ has a higher ratio. Due to donation from nitrogen, these d orbitals are expanded more in the compounds with nitrogen donor atoms. This leads to better overlap and a stronger quadruple bond.

Electron Density. We have analyzed the effect of electron correlation and the strength of the quadruple bond by comparing the electron density maps for $Cr_2(O_2CH)_4$ and $Cr_2((NH)_2CH)_4$, again at the calculated positions closest to their predicted bond length. Figure 5 shows the results at the GMO–CI level. At the

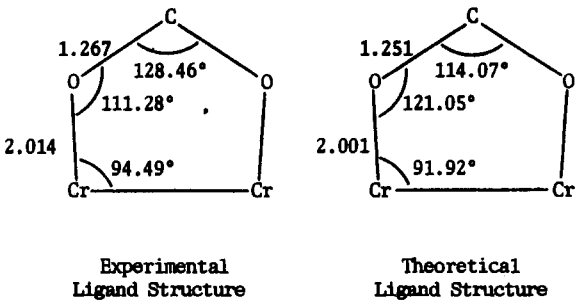

Figure 6. Comparison of theoretical vs. experimental bridging-ligand structure parameters. The values given for the theoretical structure are the ones that would have resulted if we had done a calculation at the experimental Cr–Cr bond length and our bridging-ligand arrangement.

left of the figure we have plotted the static deformation density maps, generated by subtracting spherical ground-state atoms in the same basis seet from the total electron density of the molecule. These maps show the changes in the electron density that occur when forming the molecule from its constituent atoms. The maps clearly show a buildup of density between the Cr atoms. As would be expected for multiple bonds, this buildup is elongated perpendicular to the bond direction because of strong π bonding. A comparison of the maps for these two compounds shows the much larger buildup of electron density between the chromium atoms for $Cr_2((NH)_2CH)_4$. Since each contour on these maps differs from its neighbor by a factor of 2, the buildup is significantly greater in $Cr_2((NH)_2CH)_4$.

Experimental deformation density maps have been reportedfor tetrakis(acetato)dichromium,[39] tetrakis(μ-2-hydroxy-6-methylpyridinato)dichromium,[39] and tetrakis(2,4,6-trimethoxyphenyl)-dichromium.[40] The maps for the tetraacetate showed a lack of electron density in the σ-bond region between the Cr atoms. The highest positive contour found is more in the π region and represents about 0.1 e $Å^{-3}$. On the other hand, the experimental deformation density maps for the hydroxymethylpyridine species show a strong buildup of electron density between the Cr atoms. The experimental density at the midpoint of the Cr–Cr bond is 0.41 e $Å^{-3}$ and spreads throughout the σ-, π-, and δ-bonding regions. Maps of the trimethoxyphenyl structure also show higher electron density, about 0.2 e $Å^{-3}$, slightly above and below the Cr–Cr bond. The highest positive contour in our theoretical map for the tetrakis(formato) species represent 0.05 e $Å^{-3}$, while the highest contour for the tetrakis(amino iminato) species represents 0.11 e $Å^{-3}$.

The right-hand maps in Figure 5, formed by subtracting the HF electron density from the GMO–CI electron density, show the effect of electron correlation on the density. When we add CI, the electron density is diminished in the bond region and increased close to the atoms. Although the changes in electron density when electron correlation is introduced are only a small fraction of the deformation density, they are still responsible for large changes in the bond energy.

Electron Diffraction Studies. Recently, Ketkar and Fink have reported a gas-phase electron diffraction study of $Cr_2(O_2CCH_3)_4$.[41] This study is the first report of the structure of a tetrakis(carboxylato)dichromium compound without any axial interactions. They reported a Cr–Cr bond length of 1.966 Å for this compound. This bond length is much shorter than for any other tetrakis(carboxylato)dichromium compound and places anhydrous dichromium tetraacetate almost in the range of other compounds with supershort Cr–Cr quadruple bonds. This bond length is also much shorter than the shortest value that we predict for a similar compound. In their report, Ketkar and Fink state that they cannot compare their results with theoretical computations because the computations were carried out on compounds with frozen X-ray structure parameters. At present, we are unsure whether the discrepancy between theoretical and electron diffraction results can be attributed to this difference in ligand geometry. Figure 6 compares the structural parameters for the experimentally reported compound and the values of our compound at a bond length of 1.966 Å. Although some differences exist in the bond angles, the bond lengths are virtually identical. Interestingly, it appears that the bite angle of the bridging formato group in our structure favors a short bond more than the experimental bite angle. Calculations on these compounds using the experimental structure parameters and an improved basis set are presently under way.

Conclusions

Dichromium compounds with oxygen–nitrogen bridging ligands have been synthesized containing zero, one, and two axial ligands, and these compounds do show a progressive increase in the Cr–Cr bond length that can only be attributed to axial ligand interaction. It should be noted, however, that although dichromium compounds with oxygen–nitrogen bridging ligands will take on axial ligands, the chromium to axial ligand bond length is longer than in the corresponding tetrakis(carboxylato) compounds. This indicates that these systems do not bond axial ligands as readily as tetrakis(carboxylato) species do. When attempts are made to synthesize tetracarboxylates without any axial interactions, these compounds tend to either dimerize or polymerize in order to ensure axial interactions. Yet numerous dichromium compounds with oxygen–nitrogen or nitrogen–nitrogen bridging ligands have been made without axial ligands and without dimerization taking place.

Theoretical results show that the nature of the bridging ligand strongly affects the electronic structure of the quadruple bond. Bridging ligands with donor atoms other than oxygen donate more electron density to the Cr atoms, thereby expanding the Cr 3d orbitals, causing better overlap of Cr–Cr orbitals and a stronger quadruple bond. By doing calculations on two compounds with the same symmetry, we have shown that the large change in the Cr–Cr equilibrium bond length calculated for less symmetric systems cannot be attributed totally to a calculational problem related to broken-symmetry solutions, but rather reflects the differences in the inductive effects of the formato vs. the amino iminato bridging ligand. We are presently doing calculations on species with broken-symmetry solutions to determine whether calculations on compounds of different symmetries can be directly compared.

In conclusion, this study confirms the importance of the inductive effect of the bridging ligand on the bond length of quadruply bonded dichromium(II) compounds. Although the presence or absence of axial ligands can definitely cause significant changes in the equilibrium bond length on a series of compounds with the similar bridging ligands, our results indicate that the inductive effect of the bridging ligand is also an important influence in determining the equilibrium bond length. The relative importance of these two effects is still an open question. Most theoretical workers emphasize the inductive effect of the bridging ligand, while most experimental workers view the influence of the axial ligands as most important.

Acknowledgment. This work was supported by the National Science Foundation (Grants CHE79-20993 and CHE83-09936) and the Robert A. Welch Foundation (Grant A-648). The Department of Chemistry's VAX 11/780 was purchased in part through a major instrument grant from the National Science Foundation (Grant CHE80-15792).

Registry No. $Cr_2(O_2CH)_4$, 63448-51-1; $Cr_2((NH)_2CH)_4$, 95552-77-5; Cr, 7440-47-3.

(39) Mitschler, A.; Rees, B.; Wiest, R.; Benard, M. *J. Am. Chem. Soc.* **1982**, *104*, 7501.
(40) Troup, J. M.; Extine, M. W.; Ziolo, R. F. In "Electron Distributions and the Chemical Bond"; Coppens, P., Hall, M. B., Eds.; Plenum Press: New York, 1982; p 285.
(41) Ketkar, S. N.; Fink, M. 10th Austin Symposium on Molecular Structure, Austin, TX, 1984; p 99. Ketkar, S. N.; Fink, M. *J. Am. Chem. Soc.* **1985**, *107*, 338.